

Fatigue Crack Growth Rate and Stress-Intensity Factor Corrections for Out-of-Plane Crack Growth

REFERENCE: Forth, S. C., Herman, D. J., James, M. A., and Johnston, W.M., “**Fatigue Crack Growth Rate and Stress-Intensity Factor Corrections for Out-of-Plane Crack Growth,**” *Fatigue and Fracture Mechanics: 34th Volume, ASTM STP 1461*, S. R. Daniewicz, J. C. Newman, Jr., and K. H. Schwalbe, Eds., ASTM International, West Conshohocken, PA, 2004.

ABSTRACT: Fatigue crack growth rate testing is performed using automated data collection systems that assume straight crack growth in the plane of symmetry and that use standard polynomial solutions to compute crack length and stress-intensity factors from compliance or potential drop measurements. Visual measurements used to correct the collected data typically include only the horizontal crack length, which for cracks that propagate out-of-plane, underestimates the crack growth rates. The authors have devised an approach for correcting both the crack growth rates and stress-intensity factors based on two-dimensional mixed mode-I/II finite element analysis (FEA). The approach is used to correct out-of-plane data for 7050-T7451 and 2025-T6 aluminum alloys. Results indicate the correction process works well for high ΔK levels, but fails to capture the mixed-mode effects at ΔK levels approaching threshold ($da/dN \sim 10^{-10}$ meter/cycle). Based on the results presented in this paper, the authors propose modifications to ASTM E 647: to be more restrictive on the limits for out-of-plane cracking (15 degrees); to add a requirement for a minimum of two visual measurements (one at test start and one at test completion); and to include a note on crack twisting angles, with a limit of 10 degrees being acceptable.

KEYWORDS: fatigue crack growth, mixed-mode, stress-intensity factor, aluminum, out-of-plane.

Nomenclature

a	Corrected crack length
a_c	Compliance crack length
a_n	Notch length
β	Out-of-plane angle
B	Specimen thickness
da/dN	Crack growth rate
Δa	Projected crack length
$\Delta a'$	Actual crack length
ΔK	Stress intensity factor range

¹ Materials Research Engineer, NASA Langley Research Center, MS 188E, 2 W. Reid St., Hampton, VA 23681

² Student, Washington University in St. Louis, One Brookings Drive, St. Louis, MO 63130.

³ Staff Scientist, National Institute for Aerospace, NASA Langley Research Center, MS 188E, 2 W. Reid St., Hampton, VA 23681

⁴ Research Engineer, Lockheed Martin Corporation, NASA Langley Research Center, MS 188E, 2 W. Reid St., Hampton, VA 23681

f	Out-of-plane angle fraction
K_I	Mode-I stress intensity factor
K_{max}	Maximum stress intensity factor
R	Stress ratio (minimum/maximum)
W	Specimen width

Introduction

Experimental testing for baseline fatigue crack growth rate properties has traditionally been performed on laboratory coupons designed to promote mode-I crack growth, where cracking is perpendicular to the applied load. However, material microstructure, residual stresses and other factors can cause the crack to turn out-of-plane and propagate in a mixed-mode manner. The ASTM Standard Test Method for Fatigue Crack Growth Rates (E 647), the testing standard used to develop fatigue crack growth rate data, limits the out-of-plane crack growth to within 20 degrees of the specimen symmetry plane for any growth increment over one-tenth the specimen width to maintain a reasonable accuracy of the mode-I equations. Additionally, any out-of-plane cracking exceeding 10 degrees must be reported with the data. However, in some circumstances significant numbers of specimens may be invalid because of out-of-plane cracking, or invalid by a small amount, directly impacting the value of a test program. For example, during a recent testing effort at NASA Langley Research Center on aluminum alloy 2025-T6 forgings, significant out-of-plane cracking was observed [1]. Nearly half of the test specimens had out-of-plane angles outside the ASTM E 647 limit of 20 degrees. The authors have devised an approach for correcting both the crack growth rates and stress-intensity factors based on two-dimensional mixed mode-I/II finite element analysis (FEA). The approach is used to correct out-of-plane data for 7050-T7451 obtained from the literature [2] and recent test results [1] from 2025-T6 aluminum alloys.

Mixed-Mode Crack Growth Data Correction

A correction procedure can take more than one form, depending on the format in which the data is collected. For this study, the driving force and the crack growth rate will be considered separately because the testing was controlled by an automated computer-based K-control system that used compliance to determine crack length. All crack lengths obtained during the test were computed from measured compliance. Visual measurements, taken during the test with microscopes on traveling stages, were used to correct the compliance-based crack length values after completion of the test, prior to data reporting per ASTM E 647. The visual measurements are taken along the symmetry plane of the specimen and represent the projected crack growth, Δa , defined in FIG 1. To assess the effect of mixed-mode crack growth on measured compliance values and computed stress intensity factors, finite element analyses were performed for several out-of-plane crack configurations.

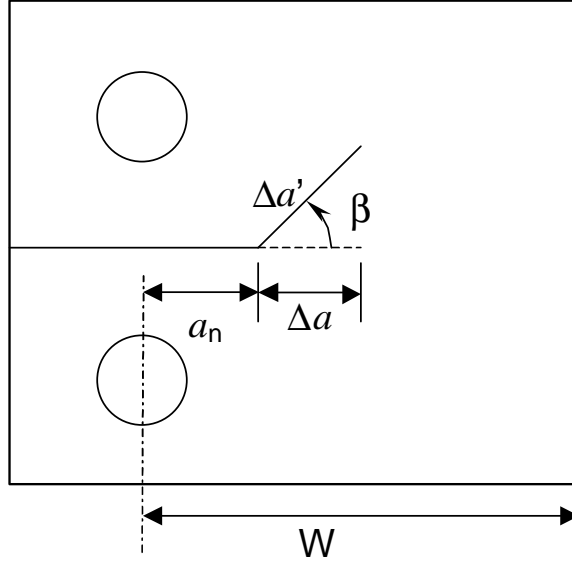


FIG 1— Out-of-plane crack growth configuration for a C(T) specimen.

Stress Intensity Factors

The finite element analysis (FEA) software FRANC2D/L [3, 4, 5] was used to calculate mode-I/II stress intensity factors (SIFs) for straight and angled crack configurations. A typical compact tension specimen, C(T), was considered with out-of-plane cracking. FIG 1 shows the configuration and nomenclature for the C(T) specimen studied herein, where the specimen dimensions for this study are: width, $W = 76.2$ mm, thickness, $B = 12.7$ mm, and notch length, $a_n = 19.05$ mm. The out-of-plane angle β was varied from 0 degrees to 40 degrees. We assumed that the precrack and subsequent crack growth was in a straight line at an angle β from the symmetry plane. In each case the projected crack growth, Δa , was kept constant at $\Delta a = 12.7$ mm and the actual crack growth $\Delta a'$ varied as

$$\Delta a' = \Delta a / \cos(\beta) \quad (1)$$

The finite element analysis was used to determine straight-crack and mixed-mode stress-intensity factors. FIG. 2 shows mixed-mode K_I SIFs normalized by the straight-crack ($\beta = 0$) SIFs as a solid line. Error bounds of $\pm 2\%$ were placed on the finite element analyses (denoted as dashed lines) for the purpose of evaluating the accuracy of the correction method to be presented. It is presumed in this paper that the K_I from the mixed-mode FEA is the most accurate representation of the SIFs at the crack tip.

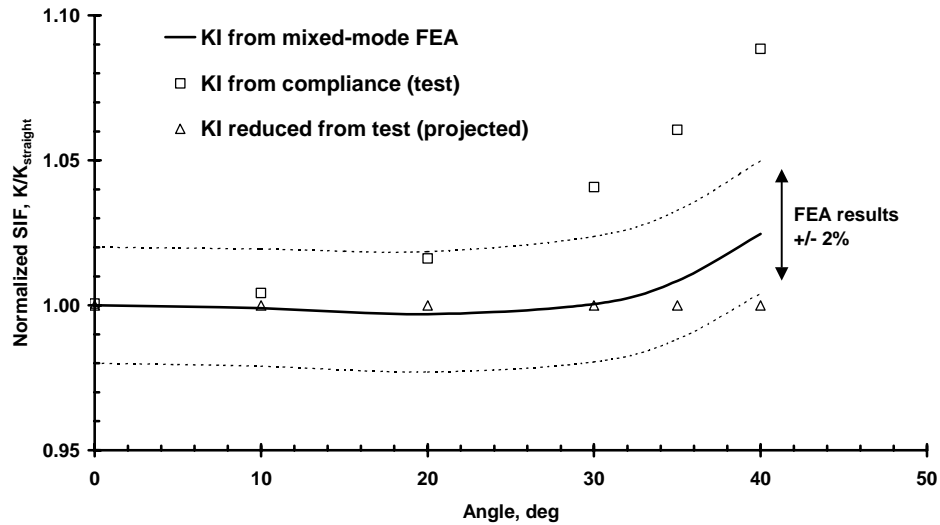


FIG. 2— Stress-intensity factor as a function of out-of-plane cracking angle.

Crack-mouth-opening displacements (CMOD) from the FEA results were used to calculate the compliance crack length and SIF values for each angle. The open squares in FIG. 2 show compliance K_I calculated from the analysis CMOD using the ASTM E 647 polynomial solutions for crack length and stress-intensity factor. The K_I from compliance is representative of the uncorrected SIF computed during a test. The compliance solution over-estimates the actual out-of-plane crack length, $a_n + \Delta a'$, resulting in a high K_I with +2% error when the crack is about 20 degrees out-of-plane and +10% error when the crack is about 40 degrees out-of-plane. The open triangles in FIG. 2 show the K_I using the projected crack length, $a_n + \Delta a$. The projected crack length SIFs are comparable to the SIFs obtained from reducing compliance data from an experiment using visual measurements. The projected crack growth underestimates the actual out-of-plane crack growth, $\Delta a'$, resulting in a reduced K_I with -2% error when the crack is about 40 degrees out-of-plane.

Using the projected crack growth to compute SIF is reasonably accurate to an angle of 40 degrees. However, the correct SIF will not be known until after the test is completed, since that is when the visual measurements will be used to reduce the compliance data. For example when conducting an experiment contained within ASTM E 647, a constant K_{max} test could no longer be valid when out-of-plane cracking occurs, as the K_{max} will vary with out-of-plane angle. However, when conducting a constant stress-ratio test, the data generated will still be at the same constant stress ratio, as both K_{max} and K_{min} vary with out-of-plane angle.

Crack Growth Rate

The crack growth rate, da/dN , should be corrected after the test is completed. Assuming the compliance data is reduced using at least two visual measurements, then the projected crack growth, Δa , is known (see FIG 1). Equation (1) must then used to determine the actual crack growth, $\Delta a'$, for computation of crack growth rate.

Correction Procedure

The stress intensity factors and crack growth rates for out-of-plane data must be corrected independently. Assuming at least two visual measurements are used to reduce the compliance data, then the SIF computed using the projected crack length, $a_n + \Delta a$, is accurate for a crack with an out-of-plane angle less than 40 degrees.

An accurate crack growth rate, da/dN , must then be computed from the projected crack growth, Δa , using equation (1).

7050-T7451 Mixed-Mode Data

Donald [2] performed tests on 7050-T7451 in the S-L orientation using compact tension, C(T), specimens. The specimens were machined such that the S-L orientation was at specific out-of-plane angles with respect to the specimen configuration, *i.e.* all crack growth was in the S-L orientation, but at different angles on the C(T) specimen, as shown in the inset of FIG. 3. Results were presented for cracking angles of 1, 10, 17 and 26 degrees and are reproduced in FIG. 3. Tests were performed at a stress ratio, R , of 0.7 and a constant ΔK of $3.3 \text{ MPa m}^{1/2}$. The results support the ASTM E 647 guidelines for out-of-plane cracking, showing that crack growth rates are affected by the out-of-plane angle.

Donald described the applied K and the projected crack length ($a_n + \Delta a$), as would be expected from the reporting requirements of ASTM E 647. The FEA results presented in FIG. 2 show that for K control based on compliance crack length, the applied K can differ significantly from the actual K at the crack tip. To apply a correction to the data, the compliance crack length must be known. An estimate of the compliance crack length can be computed from the projected crack length, since the projected crack length gives an accurate representation of the SIF for the out-of-plane angles investigated. Using the compliance crack length, we can estimate the applied load for a given ΔK , and calculate the correct crack length and subsequently a corrected ΔK . The growth rate is then corrected using equation (1) since the projected crack length is known.

Donald also provided baseline fatigue crack growth rate data over a range of ΔK values from about 2 to $5 \text{ MPa m}^{1/2}$, as shown in FIG. 3. A comparison of the average values of growth rate for uncorrected and corrected data sets with the baseline data is also presented in FIG. 3. The uppermost closed circle symbol shows the average for the 1 degree specimens. This data point is in excellent agreement with the baseline data and is not corrected. The remaining closed circles show average values for the uncorrected data. As the out-of-plane angle increases, the growth rates deviate more from the baseline data. The closed triangles show average values for the corrected data. The corrected values agree very well with the baseline data. For instance, the uncorrected, average crack growth rate for the 26 degree case is in error by 37% compared to the baseline data. The ΔK was in error by 4%. The correction of this data yielded good agreement with the baseline data, the resulting error in crack growth rate and ΔK were each less than 2%.

FIG. 4 shows the full data set for the 26 degree case. The open circles show the baseline data and the closed circles show the uncorrected out-of-plane data. The closed triangles show the data using a corrected ΔK only, *i.e.* da/dN has not been corrected. Finally, the closed squares show the corrected data. The horizontal shift in the data is the correction of SIF and the vertical shift is the correction of growth rate. The scatter in

crack growth rate and ΔK is depicted in FIG. 4 to illustrate that the uncorrected constant ΔK data masks the actual variability in the mixed-mode data. The data presented in FIG. 3 and FIG. 4 show the importance of correcting both the growth rates and driving force and the validity of this approach.

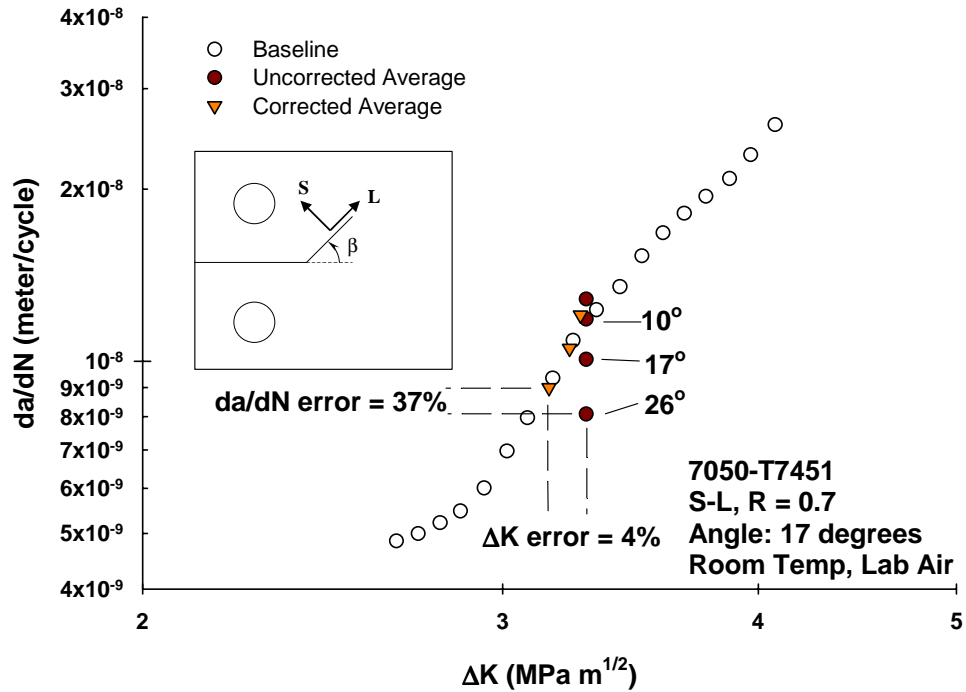


FIG. 3— Comparison of corrected data with original and baseline data.

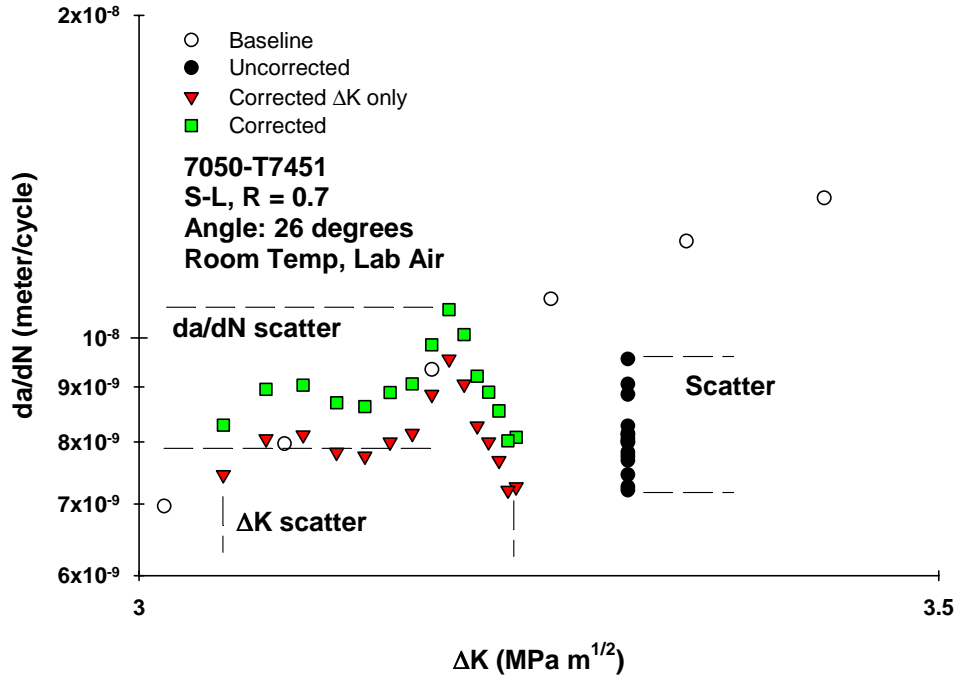


FIG. 4— Comparison of corrected data with original and baseline data for the 26 degree case.

2025-T6 Mixed-Mode Data

Test specimens were machined from near-net-shape forged aluminum alloy 2025-T6 propeller spars, shown in FIG. 5, that were provided by a propeller manufacturer. Each propeller spar is forged from cylindrical billets, so the material is substantially deformed during the forging process. The mechanical work of the forging process resulted in weak microstructural planes that promoted out-of-plane cracking, *i.e.* the microstructure directed the crack path more than the primary loading, similar to what Donald reported [2]. More information can be found in Forth, *et al* [1].



FIG. 5— Photograph of propeller spar forging made of aluminum alloy 2025-T6.

Out-of-Plane Angle

The out-of-plane angle for each specimen was determined by: (1) measuring the distance from the point at which the crack deviated from the specimen centerline to the crack tip ($\Delta a'$ from FIG 1); (2) measuring the crack growth along the specimen centerline (Δa from FIG 1); (3) computing out-of-plane angle, β , using the cosine of the two crack growth lengths measured, $\Delta a'$ and Δa . An average out-of-plane angle was then computed by averaging the out-of-plane angle measured on each side of the specimen. FIG. 6 shows the average out-of-plane angle for each of the specimens tested, and the front-to-back out-of-plane angles are presented in Table 1. For the 60 specimens, there were 16 straight cracks and 24 cracks outside the ASTM E 647 limit of 20 degrees. The remaining specimens were not straight, but were within the 20 degree limit for crack path straightness.

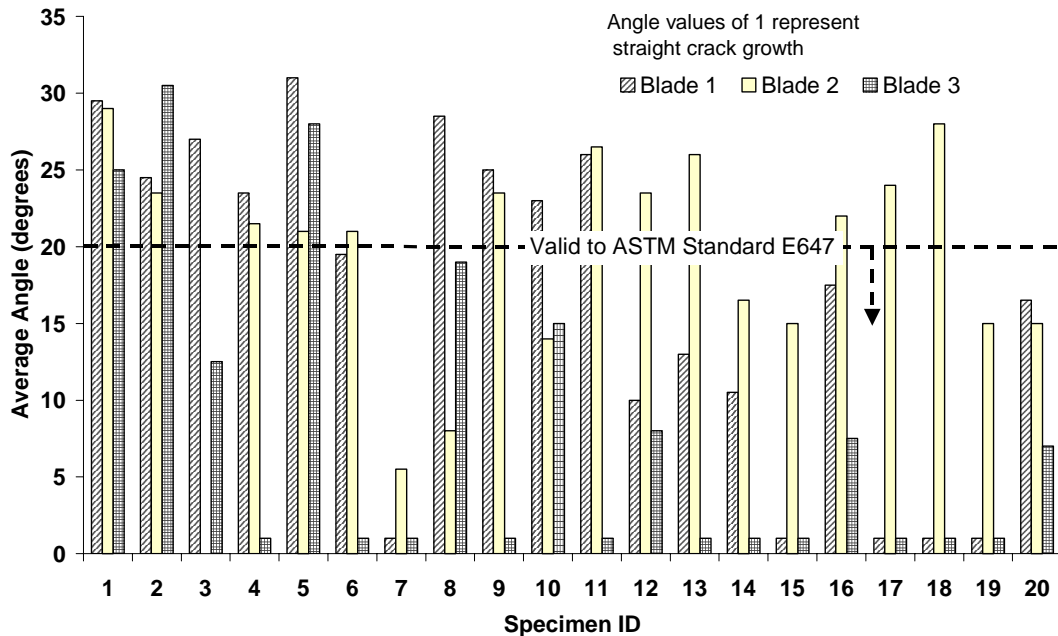


FIG. 6— Average out-of-plane angle from centerline for fatigue crack growth tests.

TABLE 1— Out-of-plane angle (front/back) from centerline for fatigue crack growth tests

Specimen ID	Blade 1 Out-of-plane angle (front/back)	Blade 2 Out-of-plane angle (front/back)	Blade 3 Out-of-plane angle (front/back)
Tip 1	31/28	26/32	25/25
2	27/22	25/22	31/30
3	25/29	untested	10/15
4	25/22	21/22	0/0
5	29/33	18/24	30/26
6	22/17	17/37	0/0
7	0/0	0/11	0/0
8	30/27	8/8	16/22
9	28/22	23/24	0/0
10	23/23	13/15	13/17

Specimen ID	Blade 1 Out-of-plane angle (front/back)	Blade 2 Out-of-plane angle (front/back)	Blade 3 Out-of-plane angle (front/back)
11	22/30	30/23	0/0
12	12/8	29/18	9/7
13	17/9	26/26	0/0
14	11/10	19/14	0/0
15	0/0	15/15	0/0
16	16/19	24/20	7/8
17	0/0	28/20	0/0
18	0/0	28/28	0/0
19	0/0	12/18	0/0
Hub 20	9/24	12/18	12/2 Hub

The specimens were numbered sequentially from the tip of the blade (1) to the hub (20), see FIG. 5, to identify trends. Two specimens were extracted across the width of the blade, such that specimens 1-b1 and 2-b1 were taken from the tip of Blade 1. High numbered specimens from Blades 1 and 3 appear to have a larger number of straight cracks, but Blade 2 did not produce any straight cracks. The specimens extracted from the hub region, which have higher specimen numbers, have less mechanical work performed on the material during the forging process, because the hub is geometrically similar to the original product form, a cylindrical billet. This led to a more uniform, orthotropic microstructure [1], decreasing the probability of a weak microstructural plane being out-of-plane with the specimen centerline, leading to more straight cracks than the tip region.

Fatigue Crack Growth Rate Data

Fatigue crack growth rate data was generated using fixed stress ratios of 0.05, 0.1 and 0.7 and using constant K_{max} values of 11, 13.7, 16.4, 22 and 33 MPa m^{1/2} per ASTM E 647. The specimen test data presented is grouped and plotted based on high and low stress ratio in FIG. 7 and FIG. 8 respectively. Specimens presented in these plots were tested using the constant R and K_{max} load reduction methods to determine threshold, $da/dN \sim 10^{-10}$ meter/cycle, and using the constant R load increasing method to determine the upper portion of the crack growth rate curve, as indicated by the figure legends. The constant R load reduction and load increasing tests are denoted with “LR” and “LI”, respectively. The specimen number is denoted in the figure legend to correlate test data to out-of-plane angle. The majority of the constant R, load increasing tests were performed following load reduction tests on the same specimen, resulting in duplicate specimen numbers in the figure legends.

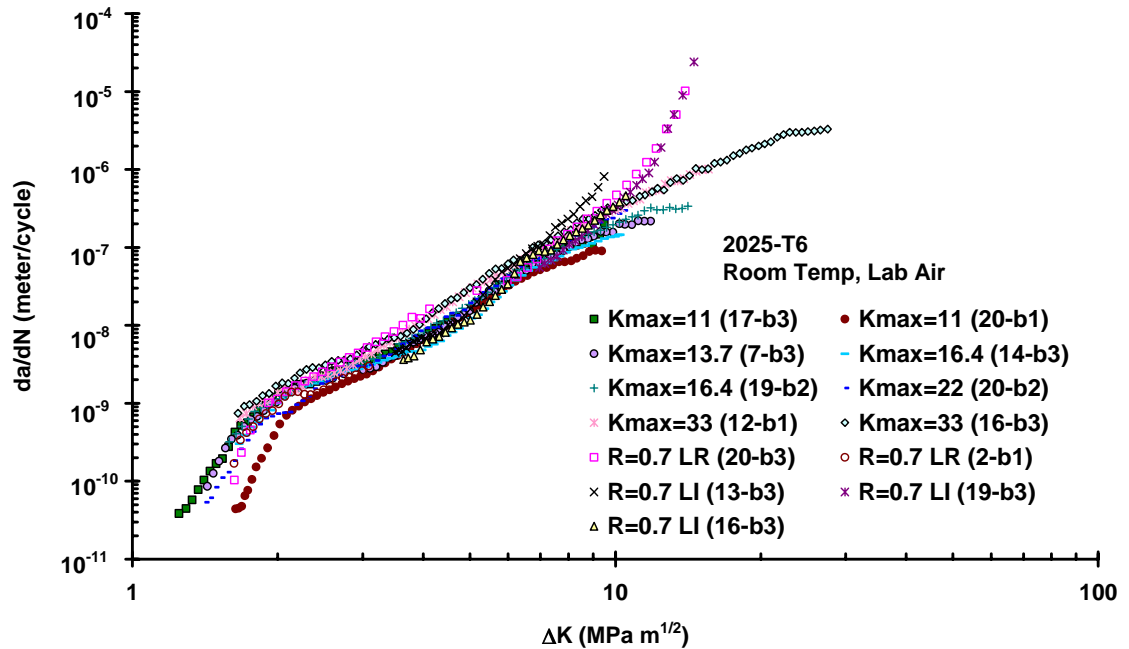


FIG. 7— High stress ratio fatigue crack growth rate data for aluminum alloy 2025-T6. (All data is corrected for out-of-plane angle.)

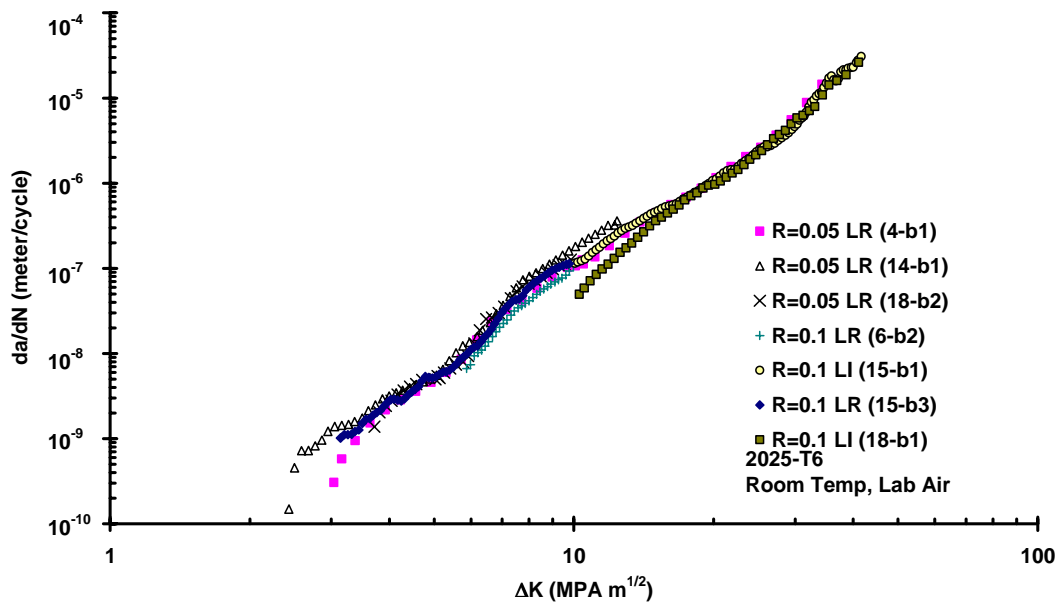


FIG. 8— Low stress ratio fatigue-crack-growth-rate data for alloy 2025-T6. (All data is corrected for out-of-plane angle.)

All of the out-of-plane data was corrected using the previously described procedure except specimens 2-b3 and 5-b1 were not analyzed because significant crack branching occurred, which is not in the realm of this correction procedure. An example of the effect that the correction procedure has on the data is presented in FIG. 9. Specimen number 18 from blade number 2 (18-b2) was chosen for examination because the average out-of-plane angle was approximately 28-degrees. The original data obtained during the test is

labeled “uncorrected.” The uncorrected data is in error with the baseline data (14-b1) by 50% in crack growth rate at a ΔK of $3.8 \text{ MPa m}^{1/2}$. The data was then adjusted for ΔK using the projected crack length. Finally, the fatigue crack growth rate was corrected to the actual crack length using equation (1) and this data set is labeled “corrected.” The correction procedure yielded slightly better agreement with the baseline data (14-b1), with an error in crack growth rate of 44% at a ΔK of $3.7 \text{ MPa m}^{1/2}$. The reduced benefit of the correction procedure at this ΔK , in comparison to Donald’s data, is discussed in the next section.

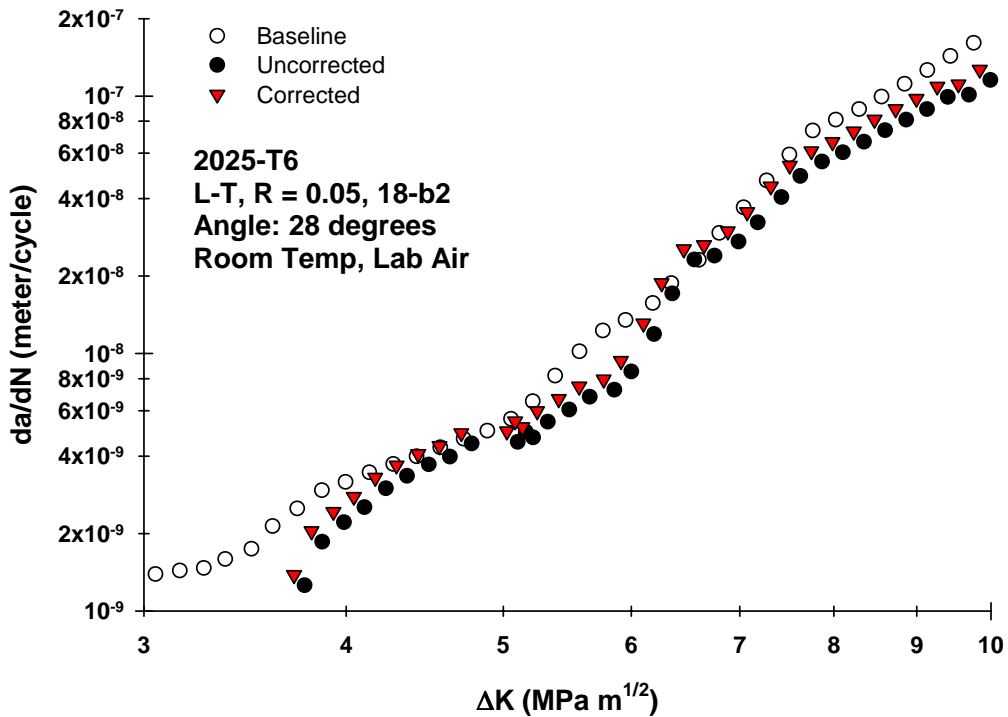


FIG. 9— Effect of corrections on the fatigue crack growth rate data of specimen 18, blade 2 ($R=0.05 \text{ LR}$).

Effect of Mode-Mixity on Crack Growth Rate

Several researches have shown experimental evidence that mixed-mode behavior at the crack tip can influence the crack growth rate [6, 7]. Based on this research, Donald [2] generated the presented data for 7050-T7451 at a stress ratio of 0.7 and a crack growth rate above 10^{-9} meters/cycle. The combination of high stress ratio and crack growth rate above threshold minimizes energy dissipation due to roughness- and plasticity-induced crack closure or other mechanisms that may influence growth rates in mixed-mode. The 2025-T6 data was generated at both high and low stress ratios and over a wide range of crack growth rates. Both the high and low stress ratio data are investigated to assess the effect mode-mixity has on fatigue crack growth. The high R data will isolate the ranges of crack growth rate that are affected while minimizing the effects of roughness- and plasticity-induced crack closure [8]. The low R data will likely

be more influenced by plasticity- or roughness-induced closure, and other mechanisms that can reduce the driving force in mixed-mode situations [7].

Focusing first on the low stress ratio data (FIG. 8), specimens 15-b1, 15-b3 and 18-b1 had out-of-plane angles of essentially zero. Specimen 14-b1 had an angle greater than 10 degrees but less than 20 degrees. These specimens comprise the data set that meet ASTM E 647, and form the basis for a low stress ratio baseline data set. The remaining three specimens are outside the 20 degree requirement. The data in FIG. 8 shows that for this data set there appears to be very little effect of out-of-plane angle for the Paris regime ($da/dN > 10^{-8}$ m/cycle for this discussion). Only two specimens approached threshold: 14-b1 and 4-b1. Specimen 14-b1 is part of the baseline set, and specimen 4-b1 had an average out-of-plane angle of about 24 degrees. Near-threshold, the out-of-plane cracking data had significantly slower crack growth. For instance, at a ΔK of approximately $3.2 \text{ MPa m}^{1/2}$ the crack growth rate of specimen 4-b1 was 6.4×10^{-10} m/cycle, whereas the baseline specimen 14-b1 had a crack growth rate of 1.4×10^{-9} m/cycle, more than a factor of two faster. Therefore, the out-of-plane angle of 24 degrees is significant near-threshold.

To investigate the high stress ratio data, constant K_{max} and constant $R = 0.7$ load reduction test specimens were chosen. The crack growth rate versus stress intensity for the constant K_{max} tests is plotted in FIG. 10. Comparing the constant $K_{max} = 11 \text{ MPa m}^{1/2}$ tests, specimen 17-b3 propagated straight whereas specimen 20-b1 propagated an average of 16.5 degrees out-of-plane (front/back = 9/24). At higher ΔK levels ($\Delta K > 5 \text{ MPa m}^{1/2}$), there is little difference in the tests. However, as the ΔK reduces below $4 \text{ MPa m}^{1/2}$, the data sets diverge with the higher out-of-plane angles having lower crack growth rates.

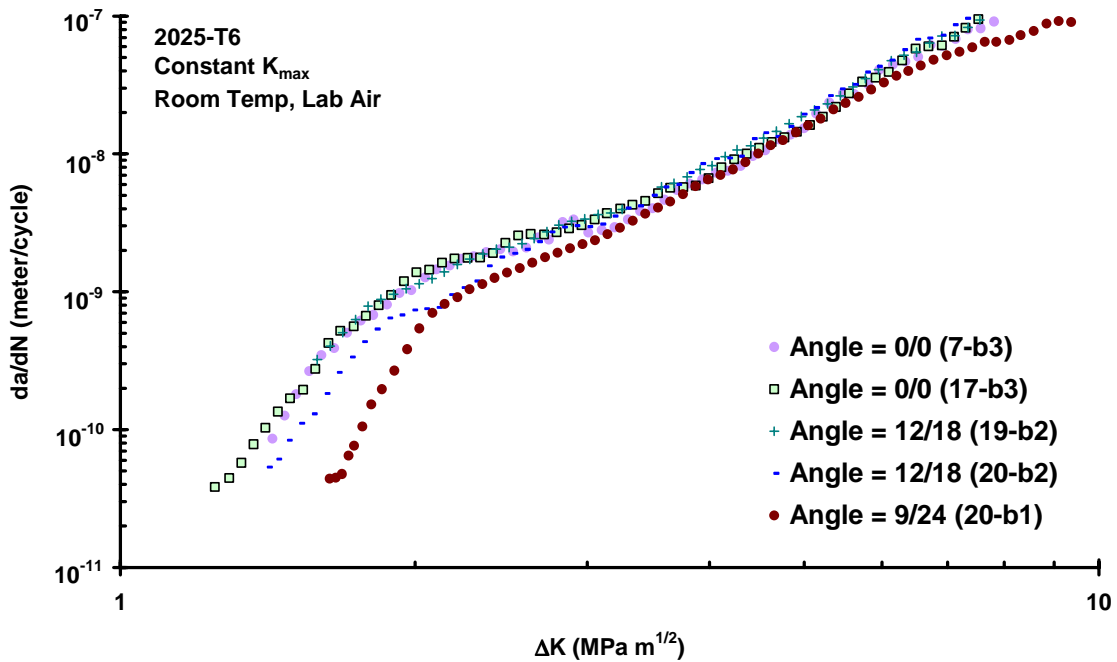


FIG. 10. Constant K_{max} data near threshold for different out-of-plane angles. (All data is corrected for out-of-plane angle.)

As a crack twists out-of-plane through-thickness for a compact tension specimen, *i.e.* twisting is defined as front-to-back out-of-plane angle variation, mode-III behavior is observed at the crack tip [9]. The difference in crack growth data from specimen 20-b1 to specimens 19-b2 and 20-b2 could be indicative of mode-III behavior. Each test propagated out-of-plane at approximately the same average angle, however specimen 20-b1 had significant twisting. Near threshold, the twisting exhibited in specimen 20-b1 translated into an order of magnitude decrease in the crack growth rate, whereas specimen 19-b2 nearly matched the straight data. Specimen 20-b2 fell between the other data and suggests that the out-of-plane angle may introduce significant variability in the crack growth rates, more than specimen 19-b2 suggests.

The constant $R = 0.7$ data is presented in FIG. 11 as crack growth rate versus stress intensity. Specimen 2-b1 propagated an average of 24.5 degrees out-of-plane. Unfortunately, there is no overlap of specimen 2-b1 data with the straight tests. However, extrapolating the data from specimen 2-b1, it would appear to have the same crack growth rates at ΔK values exceeding $5 \text{ MPa m}^{1/2}$, similar to the constant K_{max} data presented in FIG. 10. Specimen 20-b3 exhibited significant twisting, much like specimen 20-b1 discussed previously, and does overlap the straight data. Once again, the crack growth rates from specimen 20-b3 do not coincide with the straight data until ΔK exceeds $5 \text{ MPa m}^{1/2}$. A comparison of specimens 20-b3 and 2-b1 near threshold ($\Delta K < 2 \text{ MPa m}^{1/2}$) show similar crack growth behavior. It appears the effect of the high out-of-plane angle of specimen 2-b1 and the lower angle plus the twisting of specimen 20-b3 have coincidentally generated the same crack growth rates, demonstrating the significance of twisting in a low angle test.

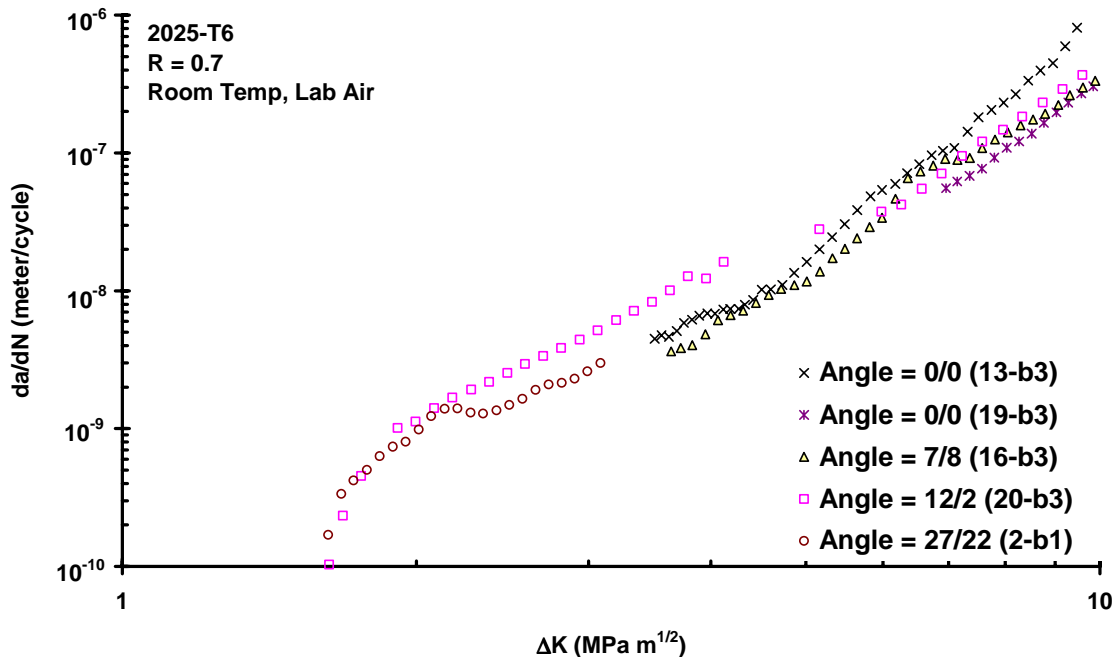


FIG. 11. Constant $R = 0.7$ data near threshold for different out-of-plane angles. (All data is corrected for out-of-plane angle.)

Discussion

When out-of-plane cracking occurs, the polynomial equations defined in ASTM E 647 under-estimate the actual crack length and over-estimate the projected crack length. This, in turn, over-estimates the stress intensity factor (SIF) and under-estimates the crack growth rates. The use of projected crack length to correct this data will correct the SIF but still underestimate the crack growth rates. These high-level continuum descriptions are only simple approximations to the true behavior along a crack front, where the crack path is not straight, but locally influenced by microstructure. The local stress intensity factor (SIF) is only a convenient approximation to the cyclic deformations that drive the growth. When compared to a straight crack, the out of plane crack likely has a more tortuous path, and the local SIFs are consequently influenced both by the global mixed-mode behavior as well as the local crack path deviations [9].

The authors have presented a very simple procedure for correcting out-of-plane crack growth data that is within 40 degrees of straight. The correction procedure was initially validated using 7050-T7451 aluminum alloy data available in the literature [2]. In that work, the out-of-plane cracking was encouraged by machining specimens with the S-L material axis rotated with respect to the crack symmetry plane of the C(T) specimen, see FIG. 3. As a result, in each case the cracking was essentially in the S-L material plane resulting in a relatively smooth and consistent fracture surface. Further, the data was generated at a high stress ratio and ΔK level to minimize crack face interaction effects. The correction procedure worked well to conform the out-of-plane data with the baseline data.

The correction procedure was also applied to out-of-plane data generated in 2025-T6 aluminum alloy from a weak microstructural plane established during the forging process. The correction procedure was applied to this data at both high and low stress ratios with some success. However, if the average out-of-plane angles exceeded 15 degrees the data could not be reliably corrected near threshold, $da/dN \sim 10^{-10}$ meter/cycle, because mixed-mode effects became dominant [10]. Furthermore, specimens that displayed significant twisting, *i.e.* the difference in out-of-plane angle measured on the specimen front and back exceeded 10 degrees, could not be reliably corrected near threshold. The authors believe that the mixed-mode behavior in the threshold regime is dominant and a simple correction procedure is inadequate.

Conclusion

In conclusion, a simple procedure has been developed to correct out-of-plane data to account for mixed-mode effects. Application of this procedure to test data that experience significant, unexpected out-of-plane cracking may aid in generating useable data. However, this procedure cannot be reliably used for crack growth rates approaching the fatigue crack growth threshold ($da/dN \sim 10^{-10}$ meter/cycle) when the out-of-plane angle exceeds 15 degrees. Furthermore, this procedure is inappropriate for correcting data that has significant variation in the through-thickness out-of-plane angle, *i.e.* twisting or mode-III type behavior. The mixed-mode phenomenon of both these cases is beyond the scope of a simple continuum-based approach to recover out-of-plane data. Finally, the ASTM E 647 standard allows for out-of-plane cracking angles to 20 degrees. Near threshold, this will lead to inaccurate data, as shown in this paper. Therefore, the standard should be more restrictive on the limits for out-of-plane cracking

(15 degrees) and add a requirement for a minimum of two visual measurements (one at test start and one at test completion) to correct for out-of-plane angles. Additionally, the standard does not address crack twisting. A note on crack twisting angles should be included, with a limit of 10 degrees being acceptable based on the data in this paper.

References

- [1] Forth, S. C., James, M. A., and Johnston, W.M., "Development and Validation of Advanced Test Methods to Generate Fatigue Crack Growth and Threshold Data for Use in Damage Tolerance Analyses," *DOT/FAA/AR-xxx*, 2003.
- [2] Donald, J. K., "The Effect of Out-of-Plane Cracking on FCGR Behavior," ASTM Research Report #E8-1001, December 12, 1995.
- [3] James, M. and Swenson, D., "FRANC2D/L: A Crack Propagation Simulator for Plane Layered Structures," Online, Available: <http://www.mne.ksu.edu/~franc2d/>, 2002.
- [4] Wawrzynek, P. A., and Ingraffea, A. R., "Integrated finite element analysis of fracture processes: an integrated approach," *Theoretical and Applied Mechanics*, No. 8, 1987, pp. 137-150.
- [5] M. A. James and D. V. Swenson, "A Software Framework for Two Dimensional Mixed Mode-I/II Elastic-Plastic Fracture," *Mixed-Mode Crack Behavior, ASTM STP 1359*, K. J. Miller and D. L. McDowell, Eds., American Society for Testing and Materials, 1999.
- [6] Lam, Y.C., "Mixed mode fatigue crack growth with a sudden change in loading direction," *Theoretical and Applied Fracture Mechanics*, Vol 19, 1993, pp 69-74.
- [7] Newman, Jr., J.C. and Piascik, R.S. (Eds.), *Fatigue Crack Growth Thresholds, Endurance Limits, and Design, ASTM STP 1372*, American Society for Testing and Materials, West Conshohocken, PA, 2000.
- [8] Smith, S.W. and Piascik, R.S., "An Indirect Technique for Determining Closure-Free Fatigue Crack Growth Behavior," *Fatigue Crack Growth Thresholds, Endurance Limits, and Design, ASTM STP 1372*, Newman, Jr., J.C. and Piascik, R.S., Eds., American Society for Testing and Materials, 2000, pp. 109-122.
- [9] Buchholz, F.G., Chergui, A. and Richard, H.A., "Fracture analyses and experimental results of crack growth under general mixed mode loading conditions," *Engineering Fracture Mechanics*, Vol. 71, 2004, pp 455-468.
- [10] Zheng, Y.S., Wang, Z.G. and Ai, S.H., "Mixed-mode I and II fatigue threshold and crack closure in dual-phase steels," *Metall. Mater. Trans. A*, Vol. 25A, No. 8, 1994, pp. 1713-1723.